NANOMATERIALS SCIENCE & ENGINEERING
Vol. 2, No. 1, pp. 35-43 (2020)

RESEARCH ARTICLE

https://doi.org/10.34624/nmse.v2i1.11209

Mechanical and Solvent Transport Characteristics of Nitro and n-Butylphenyl Supported Poly(1,3,4-Oxadiazole)s

Nimisha Kaippamangalath[1]*, Unnikrishnan Gopalakrishnanpanicker[2], Praveen C Ramamurthy[3]

[1]*Organic Nano Electronic Group, Department of Materials Engineering, Indian Institute of Science Bangalore, India*
**Corresponding author, e-mail address: nimisha.24387@gmail.com*
[2]*Polymer Science and Technology Laboratory, Department of Chemistry, National Institute of Technology Calicut, India. e-mail address: unnig@nitc.ac.in*
[3]*Organic Nano Electronic Group, Department of Materials Engineering, Indian Institute of Science Bangalore, India. e-mail address: praveen@iisc.ac.in*

Received 22 December 2019; accepted 4 March 2020; published online 10 March 2020

ABSTRACT

Examination of mechanical and solvent transport properties of π-conjugated polymers (PCPs), viz;poly(2-nitro-*p*-phenylene-1,3,4-oxadiazole) [PNPO], poly(*p*-phenylenevinylene-1,3,4-oxadiazole) [PPVO], poly(*p*-(nitrophenylene)vinylene-1,3,4-oxadiazole) [PNPVO], poly[(2-N,N'-dibutylaminophenyl)1,3,4-oxadiazole] [PNAPO], poly[pyridine(2-nitrophenyl)-1,3,4-oxadiazole] [PPNO] and poly[2-(*o*-nitrophenyl)-5-phenyl-1,3,4-oxadiazole] [PNPPO] has been done in flexible film form after blending them with poly(methylmethacrylate) or polystyrene. All six PCPs, in blended form, showed good mechanical properties with tensile strength in the range of 11.45 MPa - 22.89 MPa. Loading of TiO_2 nanoparticles onto selected polymer matrices has been found to contribute to a quantum enhancement in tensile properties. Solvent transport studies of blended polymer films and selected TiO_2 loaded matrices were carried out. Surfaces of films have been found to be predominantly hydrophobic ensuring a long service life for the appliances derived from them in moisture rich ambience.

1. INTRODUCTION

Study of mechanical and transport characteristics of macromolecules have been the key focus of many research programmes [1-2]. Mechanical properties of organic semiconductors are of critical importance during their bulk production and service period [3-4]. Despite the necessity of organic electronic materials to undergo large deformations in flexible, ultra-thin, and stretchable applications, many high-performance organic semiconductors are mechanically fragile.

Formation of composites of π-conjugated polymers (PCPs) with introduction of required amount of compatible nanoparticles into polymer matrices is a powerful approach to obtain many balanced properties by exploiting the advantages of both PCPs and nanoparticles [5-6].TiO_2 nanoparticles possess considerable mechanical strength and high surface area, and as a result, they have been widely introduced into many polymeric materials [7-8].

Synthesis, characterization and optical features of poly(2-nitro-*p*-phenylene-1,3,4-oxadiazole) [PNPO], poly(*p*-phenylenevinylene-1,3,4-oxadiazole) [PPVO], poly[*p*-(nitrophenylene) vinylene-1,3,4-oxadiazole] [PNPVO], poly[(2-N,N'-dibutylaminophenyl)1, 3, 4-oxadiazole] [PNAPO], poly[pyridine (2 - nirophenyl) 1, 3, 4 – oxadiazoe] [PPNO], and poly[2-(*o*-nirtophenyl)-5-phenyl-1,3,4-oxadiazole] [PNPPO] have been reported by us elsewhere [9-11]. The mechanical and solvent transport features of these six conjugated polymers in the flexible film form have to be explored for device applications. Along with the optoelectrical features, the mechanical strength and solvent resistant behaviour of active layers has a critical role in determining better device performance in terms of optoelectronic device life span. Based on these evaluations, a systematic investigation has been done on mechanical and solvent transport features of conjugated polymers mentioned in this manuscript. The suitability of these six macromolecules for optoelectronic device fabrication has further been confirmed through this investigation.

2. MATERIALS AND METHODS

All materials used in this work were of analytical grade. Mechanical properties of polymer films were analyzed by universal testing machine. Samples in dumb bell shape (Gauge length = 2.5 mm) were drawn with a rate of 1 mm/maccording to ASTM D-412. To study solvent resistant properties of blended films and composites, specimens of diameter 1.9 mm were prepared. Optical microscopic images were taken on Motic BA 300 optical microscope. Static contact angle measurements were performed using Drop Shape Analyzer (DSA) 100 (Kruss GmbH–Germany).

3. RESULTS AND DISCUSSIONS

Polymer films of all six PCPs were fabricated by blending strategy. Details are given in our earlier reports [9-11]. The molecular structures of six PCPs studied in this manuscript are given in Figure 1.

3.1. Mechanical properties

The mechanical properties of the blended polymer films with 2 wt% of PMMA/PS are summarized in Table 1. The tensile behaviour of the synthesized

poly(2-nitro-*p*-phenylene-1,3,4-oxadiazole) poly(p-phenylenevinylene-1,3,4-oxadiazole)

poly[*p*-(ntro phenylene)vinylene-1,3,4-oxadiazole] poly[(2-N,N'-dibutyaminophenyl)1,3,4-oxadiazole]

poly[pyridine(2-nitrophenyl)1,3,4-oxadiazole] poly [(2-(*o*-nitrophenyl)-5-phenyl-1,3,4-oxadiazole)]

Figure 1. Molecular structures of π-conjugated polymers.

PCPs is schematically illustrated in Figure 2. When a load is applied, the films (PCPs with PMMA/PS) show a yielding behaviour. This effectively helps them to accommodate the load being applied.

All films showed similar mechanical behaviour with respect to deformation under stress. Values of tensile strength are in the range of 11.45 MPa - 22.89 MPa (standard error +/-0.93128) and elongation at break in the range of 0.93 % - 3.05 %. The values are interestingly comparable or better than materials currently being used for fabrication of optoelectronic devices [12].

It has been observed that tensile properties of blends increase with increase in weight percentage of PMMA/PS from 2 wt% to 8 wt%. Typically, two polymeric systems, PNPO and PPVO with PMMA/PS, were examined to see the dependence of weight percentage of PMMA/PS and results are presented in Figure 1a and b. After 4 wt% PMMA/PS loading, all macromolecular systems exhibited emission features with low intensity [11]. Tensile properties of polymer films with PS, in each case, have been found to be higher compared to that of corresponding PMMA samples; attributed to better π-π interactions between PCPs and PS. Interestingly, comparing mechanical properties reported for poly(oxadiazole) systems synthesized earlier, present polymers exhibit higher values indicating their suitability for device fabrication [13-14], in terms of product strength and service life.

Table 1. Tensile properties of blended polymer films with 2 wt% of PMMA/PS.

Polymer Films*	**Tensile Strength (MPa)**	**Elongation at Break (%)**
PNPO/PMMA	18.10	1.08
PNPO/PS	21.12	0.93
PPVO/PMMA	16.50	0.98
PPVO/PS	17.45	2.96
PNPVO/PMMA	19.20	3.05
PNPVO/PS	19.75	2.01
PNAPO/PMMA	11.45	1.98
PNAPO/PS	15.71	1.79
PPNO/PMMA	17.50	2.60
PPNO/PS	18.30	2.10
PNPPO/PMMA	22.15	1.34
PNPPO/PS	22.89	1.20

* with 2 wt% of PMMA/PS

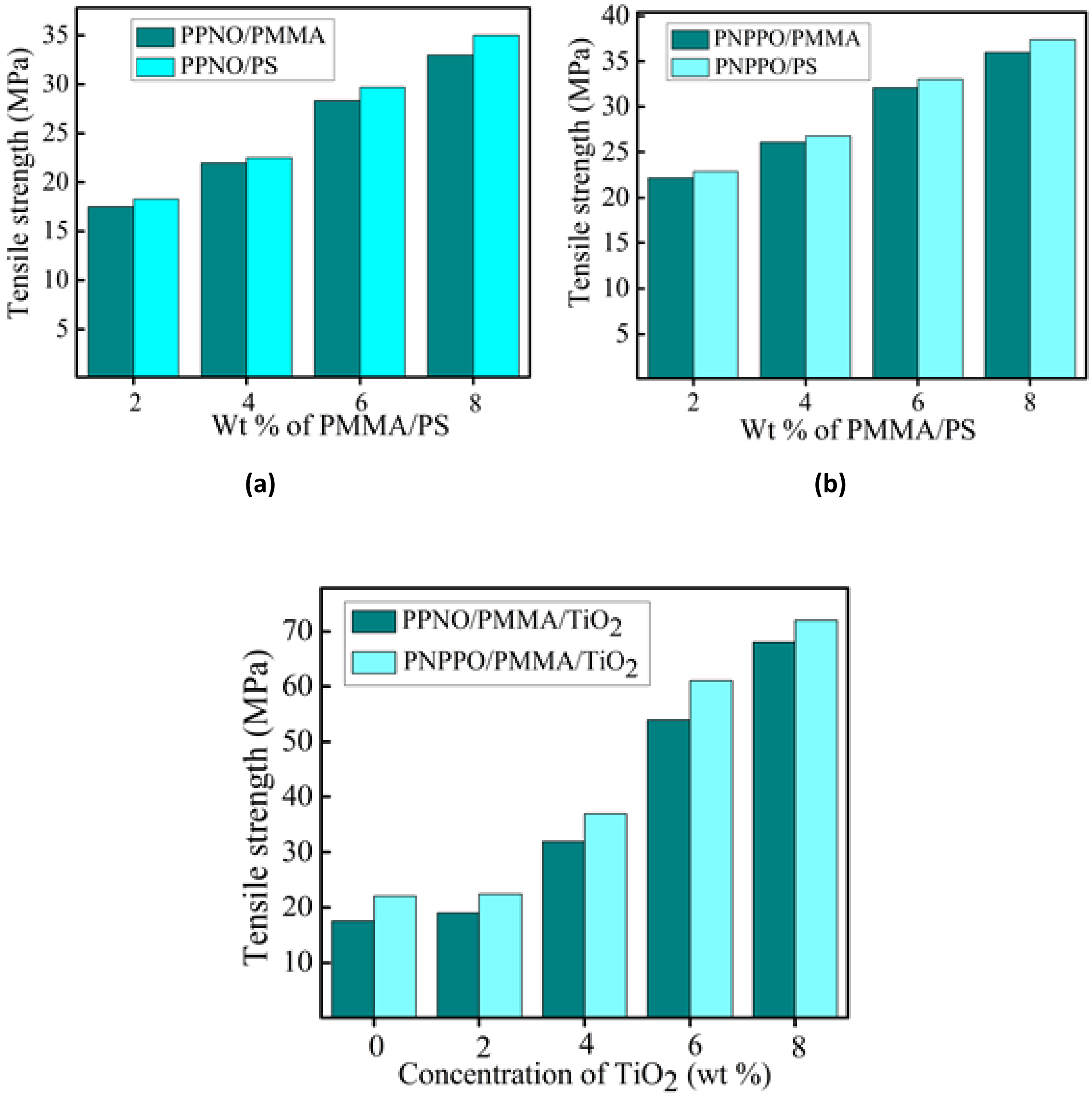

(a) (b)

(c)

Figure 2. Mechanical properties of: (a) PPNO/PMMA or PS (b) PNPPO/PMMA or PS (c) PPNO/PNPPO nanocomposites with TiO_2.

Based on our previous publication [11], we have done a detailed study of mechanical features of PPNO/PNPPO nanocomposites with TiO_2 NPs in this manuscript. The loading of TiO_2 nanoparticles into polymer matrices, typically with PPNO and PNPPO, has been found to enhance the mechanical properties significantly (Figure 2c). Mechanical properties of nanocomposites largely depend on external load transfer efficiency between nanofiller phase and matrix. Dispersion of TiO_2 NPs in polymer matrix reduces polymer-polymer interaction while increasing polymer-filler interactions. This physical reinforcement causes the system to resist applied forces, and thus tensile strength increases significantly.

Particle size and the surface area of filler play crucial role in reinforcement process. From the morphological evaluation, it has been confirmed that spherical TiO_2 nanoparticles possess average size of 50 nm [11]. The nanosized particles have large surface area which offers effective interaction with matrices [15]. Total surface area of TiO_2 filler in PCPs is directly related to the amount or percentage of weight of TiO_2 dispersed in, which accounts for the observed elevation in mechanical properties with an increase in the amount of the filler (Figure 1c). Significant enhancement of tensile strength of polymer nanocomposites can also be due to anisotropic nature of TiO_2 nanoparticles; relates to its surface activity, and thus its interaction with host matrices [16, 17].

A theoretical model, proposed by Halpin-Tsai, has been adopted to compare tensile strength of composites of PPNO/PNPPO with TiO_2. According to this model, the relative tensile strength, RTS, can be expressed as [18].

$$\text{RTS} = \frac{\sigma_c}{\sigma_b} = \frac{1+\zeta\eta_T\phi_f}{1-\eta_T\phi_f} \tag{1}$$

where η_T is given by

$$\eta_T = \frac{R_T-1}{R_T+\zeta} \tag{2}$$

and, σ_c and σ_b are tensile strength of the polymer composites and unfilled polymer systems, respectively. ϕ_f is volume fraction of TiO_2 in the polymer matrices. R_T is filler tensile strength relative to that of polymer matrix and the aspect ratio.

The volume fraction of the nanofillers distributed throughout the matrix surface has a critical value in the reinforcement of tensile strength of nanocomposites. Although, there are different theories to explain the extent of reinforcement between matrix and nanofillers, the Halpsin-Tsai model has better explained the relation between volume fraction of nanofiller, $\emptyset_f$ and tensile strength of the polymer composites, σ_c as shown in equation 1. It can be seen from Figure 3 that PNPO/PMMA/TiO_2 and PNPPO/PMMA/TiO_2 predominantly show positive deviations from theoretical predictions by Halpin-Tsai model. This observation is complementary to points discussed above, and is an indication of high filler-matrix interaction.

The tensile strength of the TiO_2 filled PPNO and PNPPO films showed an enhancement compared to their blended films with PMMA/PS. The homogeneous stress distribution in the PPNO/PNPPO based composites materials gives an improvement in strength. The theoretical values are higher than the experimental values. The increase in the deviation of theoretical values at higher TiO_2 loadings arises due to well uniform distribution of TiO_2 nanoparticles in case of low filler

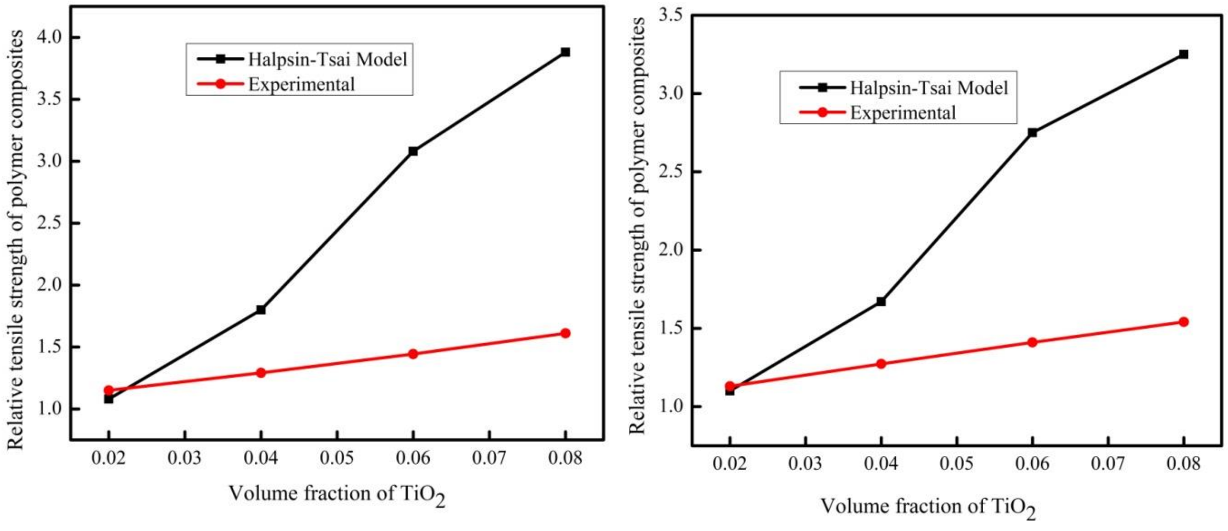

(a) **(b)**

Figure 3. Comparison of relative tensile strengths of: (a) PPNO/PMMA/TiO_2 (b) PNPPO/PMMA/TiO_2.

loadings. Also, the Halpsin-Tsai model (Equation 1) does not account into the surface area or particle size of the TiO_2 distributed in PPNO and PNPPO surfaces.

3.2. OPTICAL MICROSCOPIC ANALYSIS

In an optical microscopic technique, the enhanced scattering of light in nanostructures, due to the coupling with the surface plasmon resonance (SPR), provides a powerful strategy for imaging the location of nanoparticles (NPs) in a matrix [19]. A light source (usually white light) was focused on the PPNO/PMMA or PNPPO/PMMA surface containing strongly scattering TiO_2 NPs. The light frequencies correspond to SPR were reflected [20]. The light was then collected and imaged through a confocal microscope resulting in a colored image of the sample on a black background [21]. The wavelength of the light scattered depended on the shape and dimensions of TiO_2 NPs dispersed in the polymer matrix.

The optical microscopic images of the polymer films, PPNO/PMMA, PNPPO/PMMA and polymer nanocomposites, PPNO/PMMA/TiO_2, PNPPO/PMMA/TiO_2 are shown in Figure 4. The images confirm the homogeneous film formation

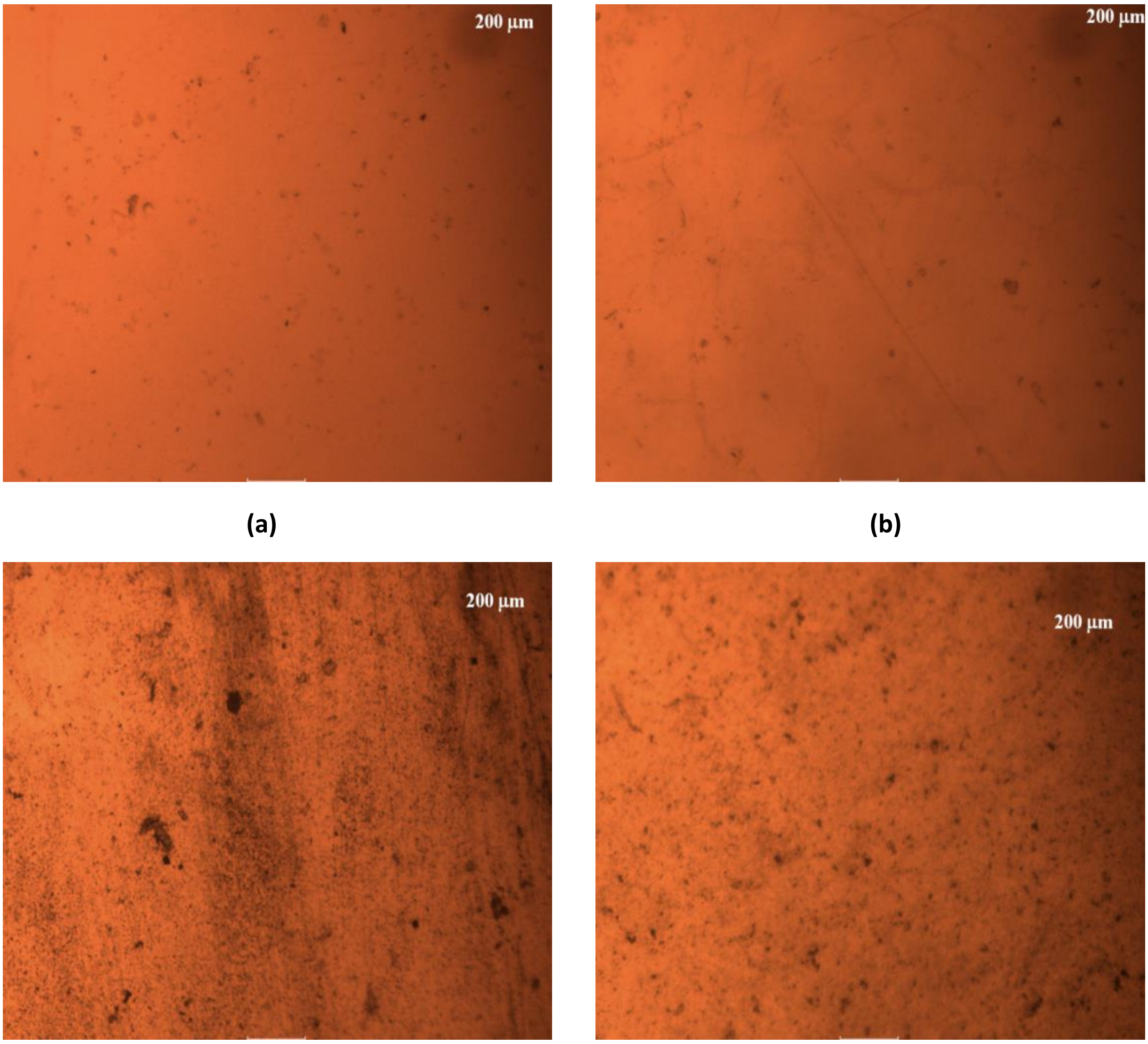

(a) (b)

(a) (b)

Figure 4. Optical images of: (a) PPNO/PMMA, (b) PNPPO/PMMA, (c) PPNO/PMMA/TiO_2 and (d) PNPPO/PMMA/TiO_2 (2 wt% TiO_2).

and the dispersion of TiO_2 nanoparticles within the matrix.

3.3. SOLVENT TRANSPORT PROPERTIES

Solvent transport properties of a PNPPO blended film with PMMA in hexane, water and ethanol media are shown in Figure 5a. No dimensional change has been noted (practically, even after many months) in water. However, in strong organic solvents viz; hexane and ethanol, film has been found to absorb penetrant after sometime.

A small weight loss was noted both in hexane and ethanol (typically after 15 hours). A comparison study on transport behaviour of a typical nanocomposite, PNPPO/PMMA/TiO_2 in hexane medium, has been illustrated in Figure 5b. In the case of NCs, the TiO_2 NPs acts superior barrier for transport of solvents. After a particular time, weight reduction of polymer blends and composites (curves pointing downward in the case of hexane and ethanol) is predominantly due to the solubility of PMMA.

An understanding of wetting behavior is very useful in the design and optimization of a wide-range of interface-sensitive optoelectronic devices and for conductive packaging material applications. Water was selected as the working liquid for contact angle measurements to characterize the wetting properties of the fabricated polymer films. The contact angle of a liquid on a textured surface θ_r^w is a function of surface roughness and the equilibrium contact angle (θ_{flat}^e) on a flat substrate of the same material. This can be expressed as [22]:

$$\cos \theta_r^w = r \cos \theta_{flat}^e \tag{3}$$

where r is the surface roughness parameter.

In the case of nanocomposites polymer films, the contact angle of liquid drop on a heterogeneous substrate in an air medium can be expressed as [23]:

$$\cos \theta_r^{CB} = f_{sl}\,(1 + \cos \theta_{flat}^e) - 1 \tag{4}$$

where, f_{sl} is the contact area fraction parameter, i.e., the ratio of the liquid–solid contact area and the projected area of the drop base.

To measure the exact value of the contact angle, the drop-substrate contact was maintained for a longer time (> 1min) to allow the drop to spread without any additional force from the needle on the drop. It is obvious from Figure 6 that the all macromolecules and their blends exhibit nearly

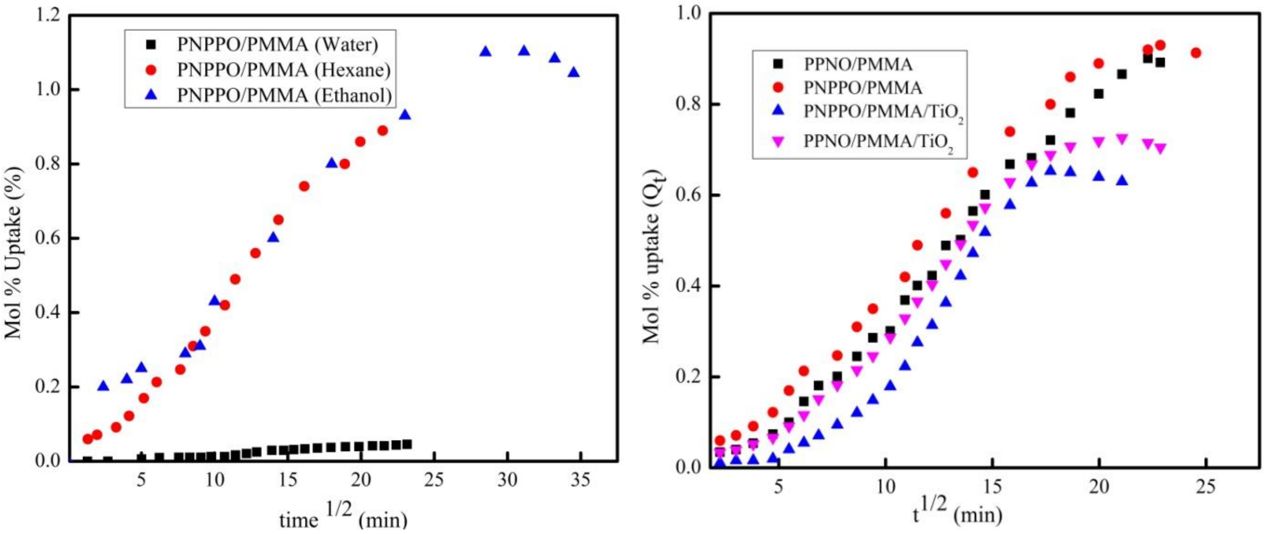

(a) **(b)**

Figure 5. Solvent transport properties through (a) blended PNPPO films (a) PNPPO composites (2 wt % TiO_2) in hexane.

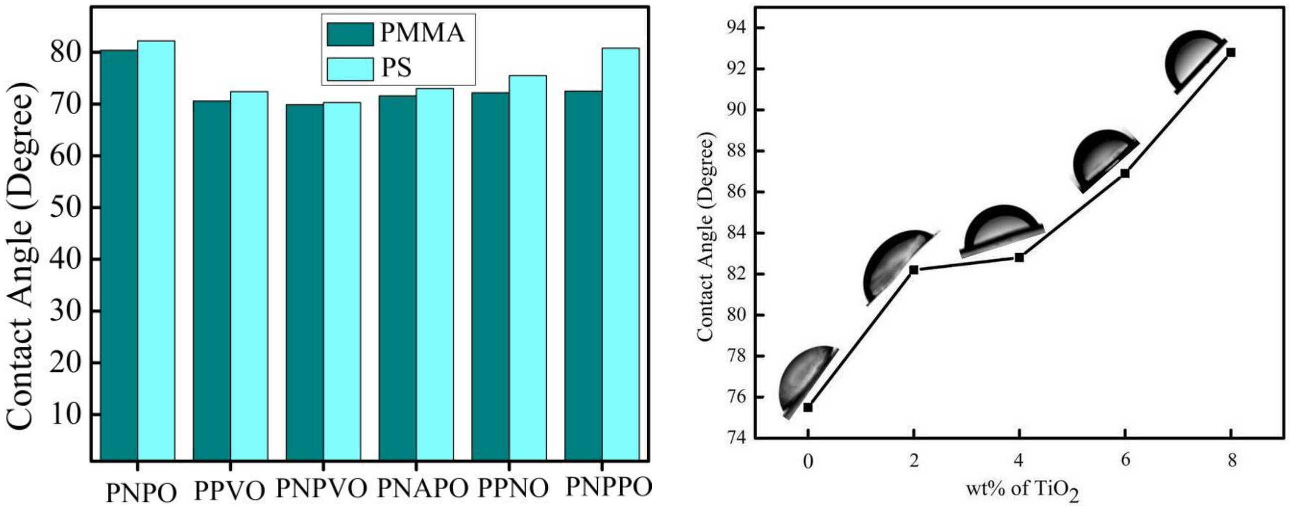

(a) **(b)**

Figure 6.(a) Contact angles of polymer blends with PMMA/PS (b) Improvement of water repelling behaviour with increase in weight percentage of TiO_2 (PNPPO/PMMA/TiO_2).

same contact angles. These values are near to the values of typical hydrophobic matrices. In all cases, the blended polymer samples with PS showed higher contact angle values than that with PMMA; resulting from the more hydrophobic nature of PS.

The water repelling behaviour of composites has also been studied with the variation of wt % of TiO_2 NPs as shown in Figure 6b. A gradual improvement in the contact angle values with increase in the wt % of TiO_2 NPs has been observed. This is attributed to the poor wetting behavior of TiO_2 nanoparticles to a range of solvents (mostly from the polar protic solvent family) [24-26]. It is well understood that the chemical heterogeneity and surface topography significantly influence the wetting characteristics of a substrate [26].

4. CONCLUSIONS

A systematic investigation on the physical properties viz; mechanical and solvent transport of the six macromolecules, poly(2-nitro-*p*- phenylene-1, 3, 4-oxadiazole) [PNPO], poly(p-phenylenevinylene-1, 3, 4-oxadiazole) [PPVO], poly[*p*-(nitrophenylene)vinylene–1,3,4-oxadiazole] [PNPVO], poly[(2-N,N'-dibutylaminophenyl)1, 3, 4-oxadiazole] [PNAPO], poly[pyridine(2-nirophenyl)-1,3,4-oxadiazoe] [PPNO], and poly[2-(*o*-nirtophenyl)-5-phenyl-1,3, 4-oxadiazole] [PNPPO] has been done in the blended and composites forms. The tensile strength values and elongation at break of the polymer films are interestingly comparable to that of the materials used as active layers in optoelectronics. The films exhibited good resistance to water. Contact angle measurements confirmed their dominant hydrophobicity. Observations presented in this work are complementary to the optical features of the new macromolecules in view of their possible utilization in optoelectronic devices and as conducting packaging materials.

ACKNOWLEDGMENTS

NK acknowledge CSIR, New Delhi, India and KSCSTE Postdoctoral fellowship.

REFERENCES

[1] Y.-S. Lee, G.-D. Sim, J.-S. Bae, J.-Y. Kim and S.-B. Lee, *Mater. Lett*. **193**, 81-84 (2017).
[2] K. Hamad, M. Kaseem, ,F. Deri and Y. G. Ko, *Mater. Lett*. **164**, 409-412 (2016).
[3] A. D. Printz, S. Savagatrup, T. N. Purdy and D. J. Lipomi, *RSC Adv*. **4**, 13635-13643 (2014).
[4] Y. Cao, P. Smith and A. J. Heeger, *Polymer***32**, 1210-1218 (1991).

[5] A. C. Balazs, T. Emrick and T. P. Russell, *Science* **314**, 1107-1110 (2006).
[6] N. Chehata, A. Ltaief, R. Bkakri and E. Beyou, *Mater. Lett.* **121**, 227-230 (2014).
[7] H. Zhang, J. Huang, X. Lin and J. Qu, *RSC Adv.* **5**, 4639-4647 (2015).
[8] X. Sui, Y. Chu and C. Liu, *Mater. Lett.* **58**, 1255-1259 (2004).
[9] N. Kaippamangalath, U. Gopalakrishnapanicker, E. Shiju and K. Chandrasekharan, *J. Mater. Sci.* **51**, 4748-4761 (2016).
[10] N.Kaippamangalath and U. Gopalakrishnapanicker, *Polym. Int.* **65**, 1221-1231 (2016).
[11] N. Kaippamangalath, U. Gopalakrishnapanicker, E. Shiju and K. Chandrasekharan, *RSC. Adv.* 6, 115132-115144 (2016).
[12] X. Lu, Z. Zhang, H. Li, X. Sun and H. Peng, *J. Mater. Chem. A* **2**, 17272-17280 (2014).
[13] M. D. Iosip, M. Bruma and P. Muller, *Eur. Polym. J.* **39**, 2011-2021 (2003).
[14] C. Hamciuc, M. Klapper and T. Pakula, *Polym. Bull.* **47**, 1-8 (2001).
[15] G. Kaur, R. Adhikari, M. Bown and P. Gunatillake, *RSC Adv.* **5**, 37553-37567 (2015).
[16] M. Wojtaś, D. V. Karpinsky, M. V. Silibin, S. A. Gavarilov, A. V. Sysa and K. N. Nekludov, *Polym. Test.* **60**, 326-332 (2016).
[17] M. Wojtas, D. V. Karpinsky, M. V. Silibin, S. A. Gavarilov, A. V. Sysa, K. N. Nekludov and S. V. Dubkov, *Polym. Test,* **71**, 296-300 (2018).
[18] J. C. Halpin and J. L. Kardos, *Polym. Eng. Sci.* **16**, 344-352 (1976).
[19] X. Huang, P. K. Jain, I. H. El-Sayed and M. A. El-Sayed, *Nanomedicine* **2**, 681-693 (2007).
[20] P. K. Jain, X. Huang, I. H. El-Sayed and M. A. El-Sayed, *Acc. Chem. Res.* **41**, 1578-1586 (2008).
[21] S. K. Brauman, *J. Polym. Sci. B* **26**, 1159-1171 (1988).
[22] A. B. D. Cassie and S. Baxter, *Trans. Faraday Soc.* **40**, 546-550 (1944).
[23] Kim, K. Noh, C. Choi, J. Khamwannah, D. Villwock and S. Jin, *Langmuir* **2011**, **27**, 10191-10196 (2011).
[24] E. Balaur, J. M. Macak, H. Tsuchiya and P. Schmuki, *J. Mater. Chem.* **15**, 4488-4491 (2005).
[25] S. Barthwal, Y. S. Kim and S.-H. Lim, *J. Colloid Interface Sci.* **400**, 123-129 (2013).
[26] S. Farsinezhad, P. R. Waghmare, B. D. Wiltshire, H. Sharma, S. Amiri, S. K. Mitra and K. Shankar, *RSC Adv.* **4**, 33587-33598 (2014).